

A novel family of insect-selective peptide neurotoxins targeting insect BK_{Ca} channels isolated from the venom of the theraphosid spider, *Eucratoscelus constrictus*

Monique J. Windley, Pierre Escoubas¹, Stella M. Valenzuela, and
Graham M. Nicholson

Neurotoxin Research Group, School of Medical & Molecular Biosciences, University of Technology, Sydney, Australia (M.J.W., S.M.V., G.M.N.); and Université de Nice Sophia Antipolis, Institut de Pharmacologie Moléculaire et Cellulaire, CNRS, Valbonne, France (P.E.)

Running Title: Novel insect-selective spider neurotoxins

Correspondence: G. M. Nicholson, School of Medical & Molecular Biosciences, University of Technology, Sydney, PO Box 123, Broadway NSW 2007, Australia. Fax: +61 2 9514 8206; Tel: +61 2 9514 2230; E-mail: Graham.Nicholson@uts.edu.au

Number of Text Pages: 31

Number of Tables: 0

Number of Figures: 8

Number of References: 39

Number of Words in Abstract: 246

Number of Words in Introduction: 655

Number of Words in Discussion: 1572

ABBREVIATIONS: 4-AP, 4-aminopyridine; 4-VP, 4-vinylpyridine; BK_{Ca} channel, large-conductance Ca²⁺ and voltage-activated K⁺ channel (K_{Ca}1.1, Maxi-K, BK, Slo1); Ca_v channel, voltage-activated Ca²⁺ channel; ChTx, charybdotoxin (α -KTx 1.1); DUM, dorsal unpaired median; EGTA, ethylene glycol-bis(2-aminoethyl ether)-*N,N,N*-tetraacetic acid; HEPES, N-hydroxyethylpiperazine-N-ethanesulfonic acid; HVA, high-voltage-activated; HXTX, hexatoxin (from the venom of spiders belonging to the family Hexathelidae); IbTx, iberiotoxin; IK_{Ca}, intermediate-conductance Ca²⁺-activated K⁺ channel (K_{Ca}3.1, IK_{Ca}1); *I*_{K(A)}, transient 'A-type' K⁺ current; *I*_{BK(Ca)}, Ca²⁺-activated K⁺ channel current; *I*_{K(DR)}, delayed-rectifier K⁺ current; α -KTx, potassium channel scorpion toxin; K_v channel, voltage-activated K⁺ channel; MALDI-TOF, matrix-assisted laser desorption/ionization time-of-flight; M-LVA, mid- to low-voltage-activated; Na_v channel, voltage-activated Na⁺ channel; NIS, normal insect saline; SK_{Ca} channel, small-conductance Ca²⁺-activated K⁺ channel (K_{Ca}2.x); SPRTX, sparatoxin (from the venom of spiders belonging to the family Sparassidae); TEA, tetraethylammonium; TRTX, theraphotoxin (from the venom of spiders belonging to the family Theraphosidae); TTX, tetrodotoxin.

ABSTRACT

Spider venoms are actively being investigated as sources of novel insecticidal agents for biopesticide engineering. Following screening of 37 theraphosid spider venoms, a family of three new ‘short-loop’ inhibitory cystine knot insecticidal toxins (κ -TRTX-Ec2a, κ -TRTX-Ec2b and κ -TRTX-Ec2c) were isolated and characterized from the venom of the African tarantula, *Eucratoscelus constrictus*. Whole-cell patch-clamp recordings from cockroach dorsal unpaired median neurons revealed that, despite significant sequence homology with other theraphosid toxins these 29-residue peptides lacked activity on insect voltage-activated sodium and calcium channels. Importantly, κ -TRTX-Ec2 toxins were all found to be high affinity blockers of insect large-conductance calcium-activated K^+ (BK_{Ca}) channel currents with IC_{50} values of 3–25 nM. In addition, κ -TRTX-Ec2a caused inhibition of insect delayed-rectifier K^+ currents, but only at significantly higher concentrations. Notably, κ -TRTX-Ec2a and κ -TRTX-Ec2b demonstrated insect-selective effects, while the homologous κ -TRTX-Ec2c also resulted in neurotoxic signs in mice when injected intracerebroventricularly. Unlike other theraphosid toxins, κ -TRTX-Ec2 toxins induce a voltage-independent channel block and therefore we propose that these toxins interact with the turret and/or loop region of the external entrance to the channel and do not project deeply into the pore of the channel. Furthermore, κ -TRTX-Ec2a and κ -TRTX-Ec2b differ from other theraphotoxins at the C-terminus and positions 5–6, suggesting that these regions of the peptide contribute to the phyla-selectivity and are involved in targeting BK_{Ca} channels. This study therefore establishes these toxins as tools for studying the role of BK_{Ca} channels in insects and lead compounds for the development of novel insecticides.

Introduction

Presently, conventional agrochemicals are used to combat phytophagous pest insects and vectors of human and livestock diseases. In addition to the issue that many have been de-registered due to human health risks and environmental concerns, one of the major dilemmas associated with these agents is the increasing development of insecticide resistance (Nicholson, 2007a). Unfortunately, wide usage and the limited target range of these compounds has resulted in an increasing incidence of insecticide resistance and a lack of effective insecticide control. Therefore there is now a push to pursue novel insect-selective compounds with alternate targets as leads for new insecticidal agents (King et al., 2008a; Nicholson, 2007b). The validation of a novel insecticidal target and insect-selective lead compounds would therefore provide a fresh approach in the development of more effective insect control agents.

It is already well established that ion channel toxins, particularly those targeting voltage-activated sodium (Na_v) channels, are useful insecticidal compounds, given their rapid lethal activity, high potency and relative insect selectivity. Nevertheless, with an increasing incidence of insecticide resistance, there is a need to explore novel targets such as insect voltage-activated calcium (Ca_v) and potassium (K_v) channels (King et al., 2008a). Importantly, potassium channels are a diverse group of ion channels represented in both electrically excitable and non-excitable tissues and as such represent a novel target mediating the effects of potential insecticidal agents.

Peptide toxins isolated from spider venoms have long been recognised as valuable pharmacological tools for probing mammalian voltage-activated ion channel structure and function (Swartz, 2007). Recently, however, attention is turning to their use as potential sources of insecticidal agents. The evolutionary process in spiders has led to the development of rich combinatorial peptide libraries mostly comprising ion channel toxins specifically designed to rapidly immobilize and kill insect prey (Escoubas, 2006; King et al., 2008a). Indeed, recent evidence would suggest that some venoms from 'primitive' mygalomorph spiders contain over 1000 peptides (Escoubas et al., 2006). While mygalomorph venoms potentially contain toxins for a wide range of insect targets, it is likely that toxins targeting voltage-activated ion channels are mainly responsible for the fast lethal effects of

these venoms in insects. It is this rapid and pernicious insect-selective activity that makes these toxins ideal candidates as leads for the design of novel insecticides.

Recently, κ -hexatoxin-Hv1c (κ -HXTX-Hv1c, formerly J-atracotoxin-Hv1c; King et al., 2008b) from the venom of the Australian funnel-web *Hadronyche versuta* (Araneae: Mygalomorphae: Hexathelidae) was identified as the first toxin to selectively and potently target an insect K^+ channel, with selective actions to block insect but not vertebrate large-conductance BK_{Ca} channels (Gunning et al., 2008). κ -HXTX-Hv1c exhibits lethal activities in a number of insect orders including Coleoptera, Diptera, Lepidoptera and Orthoptera, while lacking activity in mouse, rabbit, rat and chick preparations (Maggio and King, 2002). Thus κ -HXTX-Hv1c validates K^+ channels as potential insecticidal targets.

While several insect-selective toxins have been isolated from the venom of spiders belonging to the family Hexathelidae (for reviews see (King, 2007; Nicholson, 2007b), there has been only a limited number of investigations of insecticidal toxins from spiders of the family Theraphosidae (Corzo et al., 2008; Li et al., 2003). This is despite a number of toxins from theraphosid ('tarantula') spiders targeting mammalian ASIC, mechanosensitive, K_v , Na_v and Ca_v channels having been characterised (see the ArachnoServer 2.0 Spider Toxin Database; <http://www.arachnoserver.org/>; Herzig et al., 2011). In this study we describe a family of toxins (theraphotoxins) from the venom of the East African tarantula *Eucratoscelus constrictus* (Gerstäcker 1873; Araneae: Mygalomorphae: Theraphosidae) that block insect BK_{Ca} channels and fail to significantly affect other insect K_v , Na_v and both mid- to low-voltage-activated (M-LVA) and high-voltage-activated (HVA) Ca_v channels. Interestingly, although these toxins share their target with κ -HXTX-Hv1c they possess no obvious sequence homology, implying they may interact with distinct portions of the insect BK_{Ca} channel. These theraphotoxins will be useful for probing the biological role of BK_{Ca} channels in insects and are potential lead compounds for the development of insect-selective biopesticides.

Materials and Methods

Venom Supply. *Eucratoscelus constrictus* (formerly *E. longiceps*; see World Spider Catalog at <http://research.amnh.org/entomology/spiders/catalog/index.html>) venom was purchased from a commercial supplier (Invertebrate Biologics, Los Gatos, CA). Venom was obtained using electrical stimulation of the chelicera. Crude venom was first diluted up to $\frac{2}{3}$ of its final volume in ultrapure distilled water, centrifuged at 14,000 rpm for 30 min at 4°C and filtered using a 0.45 µm microfilter (SJGVL04NS, Millipore). The filter was rinsed with water ($\frac{1}{3}$ of final volume), the venom diluted to ten times its initial volume, and stored at –20°C until further use.

Toxin Purification and Biochemical Characterization. Bioassay-guided fractionation of *E. constrictus* venom was performed using both reversed-phase and cation-exchange high-pressure liquid chromatography (HPLC). A volume of 20–25 µl of crude venom equivalent was diluted with 0.1% aqueous trifluoroacetic acid (TFA) and fractionated by reversed-phase HPLC (RP-HPLC) on a semi-preparative C8 column (5C8MS, 10 x 250 mm, Nacalai Tesque, Japan). The column was equilibrated in 0.1% TFA, and peptides eluted with a 5–60% acetonitrile / 0.1% TFA gradient at a flow rate of 2 ml/min (see Fig. 2 for details). Fractions were collected manually by monitoring the absorbance at 215 nm. The fractions were vacuum dried, dissolved in 200 µl of ultrapure water and tested for insecticidal activity (see below). Insecticidal fractions were further purified by cation-exchange HPLC employing a TSK-gel sulfopropyl column (SP-5PW, 4.6 x 75 mm, Tosoh, Japan). The fractions were diluted to 200 µl with 20 mM ammonium acetate and were analyzed using a linear gradient from 20 mM to 2 M ammonium acetate at 0.5 ml/min (see Fig. 2 for details). Absorbance was monitored at 280 nm and fractions collected manually. Fractions were dried under vacuum, and a final purification step was undertaken using a RP-HPLC C18 column (4.6 x 250 mm, Waters Symmetry) and a water/acetonitrile /0.1% TFA gradient at 1 ml/min (see Fig. 2 for details). Purified toxins were freeze-dried and stored at –20°C.

Insect Lethality Assays. Juvenile crickets (*Gryllus bimaculatus* 3rd instar nymphs, average weight 65-70 mg) were injected intrathoracically with 1–5 µl using a 10 µl precision syringe. Samples were dissolved in distilled water and controls were injected with water only. For more rapid toxin

identification, pools of fractions were tested. Each RP-HPLC fraction (see below) was dried, reconstituted in 200 μ l distilled water and 1 μ l aliquots of each fraction were mixed to reconstitute pools of 8 to 10 fractions. Final pool volumes varied from 8 to 14 μ l depending on the number of aliquots mixed for a given pool. 2 μ l of each pool were injected into crickets as described above ($n = 3$). For individual RP-HPLC fractions, aliquots of 1 μ l were diluted ten times in distilled water and 2 μ l was injected into crickets ($n = 3$). Cation-exchange HPLC fractions were freeze-dried, redissolved in distilled water and 1/20 aliquots were injected into crickets ($n = 3$). Observation of paralysis and/or death was made at 5, 15 and 60 min post-injection with the assay endpoint for calculation of median effective doses (ED_{50}) being 15 min. ED_{50} values were evaluated using a range of 5–6 venom or toxin concentrations, with 5 crickets per dose ($n = 3$). Results were analyzed using the SOFTTOX program (SoftLabWare Inc.) employing the probit analysis method.

Mouse bioassays. Activity against vertebrates was evaluated by intracerebroventricular (ICV) injection in female C57BL/6 mice. Mice (*ca.* 20 g average weight) were lightly anesthetized with diethylether, injected in the left cerebral ventricle with 5 μ l of sample dissolved in a solution of bovine serum albumin (BSA; 2% w/v in saline) and placed in glass jars for observation. Development of signs of toxicity was noted continuously during the first hour post-injection and was monitored at regular intervals for 24 hrs or until death. A dose of 500 pmoles/mouse was used to discriminate insect-selective peptides from peptides with both insect and vertebrate activity ($n = 2$).

Edman peptide sequencing. Prior to sequencing, toxins were reduced with 20 mM β -mercaptoethanol (30 min, 37°C) and were alkylated with 4-vinylpyridine (4-VP; Wako, Japan), in 250 mM Tris-HCl/6 M guanidine buffer (pH 8.3) for 30 min at 37°C in the dark, under argon. The pyridylethylated toxins were desalted by C18 RP-HPLC using a linear gradient of acetonitrile/water/0.1% TFA. Toxin sequencing was performed on an Applied Biosystems 477A automated gas-phase sequencer (Applied Biosystems, Foster City, CA). Pyridylethylated toxins were dissolved in HPLC-grade water, applied to TFA-treated glass fiber membranes precycled with Biobrene[®] (Applied Biosystems) and subjected to N-terminal (Edman) sequencing. Sequence homologies were determined from a BLAST search of the ArachnoServer 2.0 Spider Toxin Database server.

Mass spectrometry. Mass spectra were recorded on an Applied Biosystems Voyager DE-Pro matrix-assisted laser desorption/ionization time-of-flight (MALDI-TOF) mass spectrometer (Applied Biosystems), in positive ion linear or reflector mode using α -cyano-4-hydroxycinnamic acid (α -CHCA) matrix. Calibrations were performed either in close external or internal mode, with a mixture of synthetic peptide calibrants (LaserBio Labs, Sophia-Antipolis, France). Data were analyzed with the manufacturer's DATA EXPLORER software. To confirm sequencing data, trypsin cleavage of κ -TRTX-Ec2b was performed in Tris-HCl buffer (pH 8.5) at 37°C for 4 hrs, with a 1:50 enzyme to peptide ratio. Trypsin was purchased from Promega (Charbonnières-les-Bains, France). Theoretical molecular masses were then calculated with version 7.10 of the GPMW program (<http://www.gpmaw.com/index.html>) and compared to measured masses.

Homology modeling. Three-dimensional models of the κ -TRTX-Ec2 toxins were calculated using the NMR structure coordinates of κ -TRTX-Gr2a (PDB accession 1LUP) as a template via submission to the Swiss-Model server (<http://www.expasy.ch/swissmod/SWISS-MODEL.html>) and analyzed with PYMOL software v1.3 (<http://www.pymol.org>).

Patch-Clamp Electrophysiology. Whole-cell currents were recorded in voltage-clamp mode using the whole-cell patch-clamp technique employing version 9 of the PCLAMP data acquisition system (Molecular Devices, Sunnyvale, CA). Data were filtered at 5 kHz with a low-pass Bessel filter with leakage and capacitive currents subtracted using *P-P/4* procedures. Digital sampling rates were set between 15 and 25 kHz depending on the length of the voltage protocol. Using a Flaming-Brown micropipette puller (Sutter Instruments Co., Novato, CA), single use electrodes were pulled from borosilicate glass to d.c. resistances of *ca.* 1, 1.5 and 2.5 M Ω for sodium, calcium and potassium channel current recordings, respectively. Liquid junction potentials for the various combinations of internal pipette and external bath solutions were calculated using the JPCALC software program, and all data were compensated for these values. Series resistance compensation was >80% for all cells. Cells were bathed in external solution through a continuous pressurised perfusion system at 1 ml/min, while toxin solutions were introduced via direct pressurised application via a perfusion needle at *ca.* 50

$\mu\text{l}/\text{min}$ (Automate Scientific, San Francisco, CA). All experiments were performed at ambient room temperature (20–23°C).

Primary cell culture. Dorsal unpaired median (DUM) neurons were isolated from unsexed adult American cockroaches (*Periplaneta americana*) as previously described (Gunning et al., 2008). Briefly, DUM neurons were enzymatically and mechanically isolated from the terminal abdominal ganglia of the cockroach. Extracted ganglia were removed and placed in normal insect saline (NIS) containing (in mM): NaCl 180, KCl 3.1, N-hydroxyethylpiperazine-N-ethanesulfonic acid (HEPES) 10 and D-glucose 20. Ganglia were then incubated in 1 mg/ml collagenase (type IA) for 40 minutes at 29°C. Following enzymatic treatment, ganglia were washed three times in NIS and triturated through a fire-polished pipette in order to dissociate individual neurons. The cell suspension was then distributed onto 12-mm diameter glass coverslips pre-coated with 1 mg/ml concanavalin A (type IV). Cells were maintained for no longer than 24 hrs in NIS supplemented with 5 mM CaCl_2 , 4 mM MgCl_2 , 5% FBS and 1% penicillin and streptomycin, and maintained at 30°C, 100% humidity.

Electrophysiological Recording Solutions. To record I_{Na} , the external bath solution contained (in mM): NaCl 80, CsCl 5, CaCl_2 1.8, tetraethylammonium chloride (TEA-Cl) 50, 4-aminopyridine (4-AP) 5, HEPES 10, NiCl_2 0.1, and CdCl_2 1, adjusted to pH 7.4 with 1 M NaOH. The pipette solution contained (in mM): NaCl 34, CsF 135, MgCl_2 1, HEPES 10, ethylene glycol-bis(2-aminoethylether)-N,N,N',N'-tetraacetic acid (EGTA) 5, and ATP- Na_2 3, adjusted to pH 7.4 with 1 M CsOH.

Due to the report of I_{Ca} rundown with calcium as a charge carrier and greater success when barium was used as the charge carrier (Wicher and Penzlin, 1997), BaCl_2 replaced CaCl_2 in all experiments. The external bath solution for barium current (I_{Ba}) recordings contained (in mM): Na acetate 140, TEA-Br 30, BaCl_2 3 and HEPES 10, adjusted to pH 7.4 with 1 M TEA-OH. The external solution also contained 300 nM tetrodotoxin (TTX) to block Na_v channels. Pipette solutions contained (in mM): Na acetate 10, CsCl 110, TEA-Br 50, ATP- Na_2 2, CaCl_2 0.5, EGTA 10 and HEPES 10, adjusted to pH 7.4 with 1 M CsOH.

The external bath solution for recording macroscopic K_v channel currents contained (in mM): NaCl 150, KCl 30, CaCl_2 5, MgCl_2 4, TTX 0.3, HEPES 10 and D-glucose 10, adjusted to pH 7.4 with

1 M NaOH. The pipette solution consisted of (in mM): KCl 135, KF 25, NaCl 9, CaCl₂ 0.1, MgCl₂ 1, EGTA 1, HEPES 10 and ATP-Na₂ 3, adjusted to pH 7.4 with 1 M KOH.

To eliminate any influence of differences in osmotic pressure, all internal and external solutions were adjusted to 400 ± 5 mosmol/l with sucrose. Experiments were rejected if there were large leak currents or currents showed signs of poor space clamping.

Curve-Fitting and Statistical Analysis. Data analyses were completed off-line at the conclusion of experiments using AXOGRAPH X version 1.1 (Molecular Devices). Mathematical curve fitting was accomplished using PRISM version 5.00b for Macintosh (GraphPad Software, San Diego CA, USA). All curve-fitting routines were performed using non-linear regression analysis employing a least squares method. Comparisons of two sample means were made using a paired Student's *t*-test. Multiple comparisons were assessed by repeated measures analysis of variance with a Bonferroni's multiple comparison post-hoc test; differences were considered to be significant if *p* < 0.05. All data are presented as mean ± standard error of the mean (SEM) of *n* independent experiments, unless stated otherwise.

The following equation was employed to fit current-voltage (*I-V*) curves:

$$I = g_{\max} \left(1 - \left(\frac{1}{1 + \exp[(V - V_{1/2})/s]} \right) \right) (V - V_{\text{rev}}) \quad \text{Equation 1}$$

where *I* is the amplitude of the peak current (either *I*_{Ba}, *I*_{Na} or *I*_K) at a given test potential *V*, *g*_{max} is the maximal conductance, *V*_{1/2} is the voltage at half-maximal activation, *s* is the slope factor, and *V*_{rev} is the reversal potential.

Concentration-response curves were fitted using the following Logistic equation:

$$y = \frac{1}{1 + ([x]/IC_{50})^{n_H}} \quad \text{Equation 2}$$

where *x* is the toxin dose, *n*_H is the Hill coefficient (slope parameter), and *IC*₅₀ is the median inhibitory concentration to block channel currents.

Results

Purification of insecticidal neurotoxins. As part of a search for novel insecticidal peptide toxins, a large scale screening of theraphosid venoms was pursued. Venom extracted from the African ‘tarantula’ *E. constrictus* was selected for its particularly potent paralytic activity in crickets ($ED_{50} = 0.017 \mu\text{l/g}$; Fig. 1). Bioassay-guided fractionation of crude *E. constrictus* venom by C8 RP-HPLC yielded 26 fractions, with fraction 14 (*f*14) being selected for its high insecticidal toxicity (Fig. 2A). As fractions *f*14 to *f*16 were inadequately resolved in the first HPLC separation, they were pooled and analyzed together by cation-exchange HPLC (Fig. 2B). This led to the separation of seven fractions (*f*14.1-*f*14.7) that were then tested for insect and mammalian activity. These seven fractions yielded three insecticidal peptides (*f*14.2, *f*14.3, *f*14.5), which were fully purified after an additional chromatography step using C18 RP-HPLC (Fig. 2C). In the insect assay, all three fractions demonstrated significant neurotoxicity at a dose of 1.1 nmol/g (4 $\mu\text{g/g}$). At this dose, the three toxins caused rapid insecticidal activity, with complete paralysis within 5 min, and death within 15 min ($n = 3$). For *f*14.2 and *f*14.3, ICV injection of 500 pmoles (1.8 μg) into 20 g mice ($n = 2$) also did not result in any neurotoxicity or behavioral symptoms. All aspects of mouse posture and behavior appeared to be totally unaffected by toxin injection, indicating that *f*14.2 and *f*14.3 are phyla-selective neurotoxins. Conversely, injection of 500 pmoles of *f*14.5 (1.8 μg) into 20 g mice ($n = 2$) resulted in strong neurotoxicity symptoms including convulsions, tonic paralysis, general ataxia, extension of legs and toes, tail erection and respiratory paralysis resulting in very marked cyanosis of the animal. These symptoms appeared to be reversible as animals recovered from cyanosis and tonic paralysis after *ca.* 4 hrs, and started to resume normal posture and activity.

Edman degradation of reduced and alkylated peptides yielded the complete N-terminal sequence of the three toxins from single sequencing runs. All cysteine residues were definitively established following reduction and alkylation using 4-VP. Based on their mass and amino acid sequence, these toxins belong to a class of inhibitory cystine knot (ICK) toxins (Pallaghy et al., 1994) with six cysteines (C_I - C_{VI}). The κ -TRTX-Ec2 toxins also clearly belong to the family of ‘short-loop’ ICK

spider peptides, distinguished from the more common 'long-loop' ICK spider toxins, by the presence of only three residues in the C_V-C_{VI} loop (Escoubas and Rash, 2004). Due to high homology with a number of other previously characterised 'short-loop' tarantula, we propose the presence of three disulfide bonds (Fig. 3A) linked in the C_I-C_{IV}, C_{II}-C_V, C_{III}-C_{VI} pattern resulting in a disulfide-linked pseudo-knot previously described for this toxin family.

In order to verify sequencing data, *f14.3* was also digested with trypsin and the resulting peptide mixture analysed with MALDI-TOF mass spectrometry, for confirmation of sequence ambiguities, particularly the presence of Trp²⁴. In addition, the measured masses of the peptides were matched with calculated theoretical mass values of the amino acid sequence, using the software program GPMW. This allowed complete unambiguous sequence confirmation (data not shown).

Each peptide consists of 29 amino acids with observed monoisotopic molecular weights of 3626.73, 3676.71 and 3627.16 Da for *f14.2*, *f14.3* and *f14.5*, respectively. This compares very well with the monoisotopic mass predicted from the sequence of 3626.53, 3676.51 and 3627.52 Da, respectively. This indicates that there are no apparent post-translational modifications, such as C-terminal amidation, observed with certain other spider toxins (eg. β -TRTX-Gr1b, formerly GsAFI; see Fig. 3A). The three toxins share greater than 80% sequence homology with a number of spider toxins, the majority of which are short-loop toxins from the venom of another short-loop theraphosid spider, *Grammostola rosea* (Fig. 3A). Homologous peptides exhibited a range of activities including high affinity inhibition of Na_v, Ca_v1.2, Ca_v3.1, K_v4.1, K_v4.2, K_v4.3 and K_vAP channels and weak affinity for mechanosensitive and K_v2.1 channels (see the ArachnoServer 2.0 Database for a full list of references). Furthermore, the positions of all cysteines were strictly conserved with all short-loop theraphosid spider toxins (Fig. 3A).

Using the rational nomenclature system for spider toxins proposed by King *et al.* (2008), *f14.2*, *f14.3* and *f14.5* were named κ -theraphotoxin(TRTX)-Ec2a, κ -TRTX-Ec2b and κ -TRTX-Ec2c, respectively. The activity descriptor prefix ' κ ' indicates modulators of K⁺ channels (evidence presented below), 'theraphotoxin' is the generic name for toxins from the family Theraphosidae (see Table 4 in the Supplementary data within King *et al.*, 2008b), 'Ec' is the genus and species descriptor

for *Eucratosceles constrictus*, '2' is consistent with the majority of other short-loop ICK 'tarantula' toxins (see below), and 'a', 'b' and 'c' denote the first three paralogs (isoforms) discovered.

Target determination of κ -TRTX-Ec2 toxins. While κ -TRTX-Ec2 toxins share a similar sequence and cysteine spacing arrangement with short-loop theraphotoxins this provided few clues as to the potential target of κ -TRTX-Ec2 toxins. This is because within the short-loop theraphotoxin group, the biological activities are quite diverse with activities on a wide variety of voltage-activated and mechanosensitive ion channel targets. Nevertheless, given the considerable sequence homology of κ -TRTX-Ec2 toxins with β -TRTX-Gr1a (formerly GrTx-I) from *Grammostola rosea* (Fig. 3A), a toxin known to target mammalian Na_V channels, initial experiments investigated if κ -TRTX-Ec2 toxins modulated insect Na_V channel currents (I_{Na}). Whole-cell tetrodotoxin(TTX)-sensitive I_{Na} were recorded from cockroach DUM neurons in the voltage-clamp configuration. Test pulses to -10 mV (Fig. 4D) from a holding potential (V_h) of -90 mV elicited a fast activating and inactivating inward I_{Na} that could be abolished by addition of 300 nM TTX (Fig. 4A). Application of 330 nM κ -TRTX-Ec2b failed to significantly alter I_{Na} amplitude or timecourse over a 10-min perfusion period ($92 \pm 4\%$ of control peak I_{Na} , $p > 0.05$, $n = 3$; Fig. 4A).

Experiments then investigated whether κ -TRTX-Ec2 toxins modulated the activity of insect Ca_V channels. This was based on their significant sequence homology with $\tilde{\beta}\omega$ -TRTX-Tp2a (formerly ProTx-II) from *Thrixopelma pruriens* (Fig. 3A) previously shown to target mammalian $\text{Ca}_V1.2$ and $\text{Ca}_V3.1$ channels, as well as Na_V channels (Edgerton et al., 2007; Middleton et al., 2002). We investigated the action of κ -TRTX-Ec2 toxins on both high-voltage-activated (HVA) and mid- to low-voltage-activated (M-LVA) Ca_V channels that have been previously characterised in cockroach DUM neurons (Chong et al., 2007). Unfortunately, despite differences in the kinetic and pharmacological properties of M-LVA and HVA Ca_V channels, there remains no mechanism for recording one current in isolation from the other as no peptide or organic blockers are available that exclusively block one channel subtype. As previously described, depolarizing pulses to two potentials (-20 mV and $+30$ mV; Fig. 4D) from a V_h of -90 mV were used to investigate the actions of the κ -TRTX-Ec2 toxins on M-LVA and HVA Ca_V channels, respectively (Chong et al., 2007). The elicited barium current (I_{Ba}) was

abolished by addition of 1 mM CdCl₂, confirming that currents were carried via Ca_v channels (Fig. 4Ba). A 10-min application of 330 nM κ-TRTX-Ec2b failed to significantly reduce either M-LVA or HVA Ca_v channel currents, with only a 10 ± 6% (*p* > 0.05, *n* = 3) and 7 ± 6% (*p* > 0.05, *n* = 3) inhibition of control peak *I*_{Ba}, respectively (Fig. 4Ba and Bb).

To determine if κ-TRTX-Ec2 toxins alter the voltage-dependence of channel activation, voltage protocols from a *V*_h of -90 mV to +70 mV in 10-mV increments were delivered at a frequency of 0.1 Hz to elicit families of *I*_{Na} and *I*_{Ba}. Resultant peak *I*_{Na}-*V* and peak *I*_{Ba}-*V* relationships were fitted with Equation 1 (Materials and Methods). Consistent with a lack of inhibition of *I*_{Na} or *I*_{Ba} amplitude, there was no significant shift in the threshold, or voltage midpoint, of activation (*V*_{1/2}) of Na_v or Ca_v channels in the presence of 330 nM toxin (data not shown). These experiments therefore indicate that κ-TRTX-Ec2 toxins fail to affect invertebrate Na_v and Ca_v channels in the model studied.

Global K_v channel currents were recorded in the presence of 300 nM TTX and 1 mM CdCl₂ to block Na_v and Ca_v channel currents, respectively. Currents were elicited by depolarizing test pulses to +30 mV (Fig. 4D) and upon addition of 50 mM tetraethylammonium(TEA) chloride, a non-selective K_v blocker, the channel current was completely abolished indicating that these currents were carried by K⁺ channels (data not shown). In contrast to the lack of overt activity on insect Ca_v and Na_v channels, a 10 min perfusion with 330 nM κ-TRTX-Ec2a, -Ec2b or -Ec2c resulted in a significant reduction in DUM neuron global K_v channel current amplitude (Fig. 4C). This effect was partially reversible with *ca.* 50% recovery observed following a 10 min washout with toxin-free external solution.

Determining the K⁺ channel subtype specificity of κ-TRTX-Ec2 toxins. Block of global outward *I*_K indicates that κ-TRTX-Ec2 toxins target at least one of the four major K⁺ channel current subtypes in cockroach DUM neurons. These are identified according to their current kinetics and pharmacological properties and include slowly activating, non-inactivating delayed-rectifier (*I*_{K(DR)}), transient 'A-type' (*I*_{K(A)}), transient Na⁺-activated (*I*_{K(Na)}), as well as large-conductance 'late-sustained' and 'fast-transient' Ca²⁺-activated (*I*_{BK(Ca)}) K⁺ channel currents (Grolleau and Lapied, 1995). The fast-transient BK_{Ca} channel differs from the late-sustained BK_{Ca} channel in that it inactivates rapidly after

activation and displays a voltage-dependent resting inactivation (Grolleau and Lapied, 1995). The K_{Ca} current in cockroach DUM neurons is of the large-conductance (BK_{Ca}) subtype since the current is voltage-activated, whereas SK_{Ca} and IK_{Ca} channel currents are voltage-insensitive, and no apamin-sensitive SK_{Ca} channels have been found in isolated cockroach DUM neurons (Grolleau and Lapied, 1995). As a consequence of the inhibition of macroscopic outward I_K , all subtypes except K_{Na} channels, which contribute only a minor portion of the total current, were investigated as potential targets of κ -TRTX-Ec2 toxins.

For isolation of K^+ channel subtypes, various channel blockers and current subtraction routines were utilised. In order to isolate outward $I_{K(DR)}$ in DUM neurons, $I_{K(A)}$ were blocked with 5 mM 4-aminopyridine (4-AP) (Grolleau and Lapied, 1995; Gunning et al., 2008) while BK_{Ca} channels were blocked with 1 mM $CdCl_2$ and 30 nM charybdotoxin (ChTx) (Gunning et al., 2008). Both κ -TRTX-Ec2b and κ -TRTX-Ec2c (330 nM) failed to significantly inhibit $I_{K(DR)}$ ($p > 0.05$, $n = 3$; Figs. 5Cb, 5Cc). However κ -TRTX-Ec2a produced a 31 ± 12 % inhibition of control $I_{K(DR)}$ ($p < 0.01$, $n = 3$; Fig. 5Ca). To assess whether κ -TRTX-Ec2 toxins alter the voltage-dependence of $I_{K(DR)}$ activation, the current-voltage ($I_{K(DR)}-V$) relationship in the presence of each toxin was determined using a series of 100 ms voltage pulses from a V_h of -90 mV to $+40$ mV in 10-mV increments, delivered at a frequency of 0.2 Hz. The threshold of $I_{K(DR)}$ activation was at membrane potentials more depolarised than -50 mV, in agreement with previous data from $I_{K(DR)}$ recordings in DUM neurons (Grolleau and Lapied, 1995; Gunning et al., 2008). Data were normalised against maximal late current (measured at 100 ms) recorded in the absence of toxin, and subsequently fitted with Equation 1 (Materials and Methods). Importantly there were no significant shifts in the voltage-dependence of $I_{K(DR)}$ activation for any κ -TRTX-Ec2 toxin ($\Delta V_{1/2} < 5.5$ mV for all toxins, $p > 0.05$, $n = 3-7$; Fig. 5D). In summary, κ -TRTX-Ec2b and κ -TRTX-Ec2c failed to significantly inhibit $I_{K(DR)}$, although in the case of κ -TRTX-Ec2a this may account for a statistically significant proportion of the block of global K_V current (Fig. 4C).

In insects, the *shaker*, *shab*, *shaw* and *shal* genes encode for the equivalents of mammalian K_{V1} - K_{V4} channels, respectively. While it is believed the Shab and Shaw channels are responsible for $I_{K(DR)}$ in insects (Wei et al., 1990) little work has been done on native neurons, apart from *Drosophila*, to

determine the various contributions of these two channels. Therefore, it is quite possible that κ -TRTX-Ec2a targets, with moderate affinity, one of the two possible K_V channel subtypes contributing to $I_{K(DR)}$. However, at present, the relative expression of Shab vs. Shaw channel subtypes in cockroach DUM neurons is unknown and given the potent action on BK_{Ca} channels (see below) such an action is unlikely to contribute significantly to the overall activity of κ -TRTX-Ec2a.

Of particular interest was the effect of κ -TRTX-Ec2 toxins on $I_{K(A)}$ due to their homology with a number of theraphosid spider toxins targeting the mammalian K_V4 channel (Fig. 3A). The K_V4 channel is the ortholog of the insect Shal channel that is believed to underlie a significant portion of the $I_{K(A)}$ (Salkoff et al., 1992). $I_{K(A)}$ cannot be recorded in isolation from $I_{K(DR)}$ because there are no selective blockers of insect $I_{K(DR)}$. To record $I_{K(A)}$ in isolation from other K_V channel currents a subtraction routine was therefore employed utilizing 4-AP. To isolate $I_{K(A)}$, neurons were continuously perfused with 30 nM ChTx and 1 mM $CdCl_2$ to block BK_{Ca} channels (Gunning et al., 2008). At the conclusion of experiments, 5 mM 4-AP was then perfused to eliminate $I_{K(A)}$, allowing for offline subtraction of the remaining $I_{K(DR)}$. Experimentally, this involved separate experiments with κ -TRTX-Ec2a, -Ec2b or -Ec2c which were perfused for a period of 10 minutes or until equilibrium was achieved. 5 mM 4-AP was then applied to block $I_{K(A)}$. The remaining $I_{K(DR)}$, recorded in the presence of 4-AP, was then digitally subtracted from both controls and currents recorded in the presence of each κ -TRTX-Ec2 toxin. While there was a small reduction in the amplitude of $I_{K(A)}$ in the presence of κ -TRTX-Ec2a, $I_{K(A)}$ at +30 mV were not significantly reduced by any of the κ -TRTX-Ec2 toxins, ($p > 0.05$, two-way ANOVA, $n = 3$; Fig. 5A). To assess whether κ -TRTX-Ec2 toxins alter the voltage-dependence of $I_{K(A)}$ channel activation, the current-voltage ($I_{K(A)}$ - V) relationship in the presence of each toxin was determined using the same voltage protocol as for $I_{K(DR)}$ - V curves. Again, in agreement with previous data from $I_{K(A)}$ recordings in DUM neurons, the threshold of $I_{K(A)}$ activation was at membrane potentials more depolarised than -50 mV (Grolleau and Lapied, 1995; Gunning et al., 2008). Importantly there were no significant shifts in the voltage-dependence of K_A channel activation for any κ -TRTX-Ec2 toxin ($\Delta V_{1/2} < 5.5$ mV for all toxins, $p > 0.05$, $n = 3-7$; Fig. 5B). In summary, the

κ -TRTX-Ec2 toxins failed to inhibit $I_{K(A)}$ to an extent that could account for the 20–40% decrease seen in global K_V currents (Fig. 4C).

Like $I_{K(A)}$, BK_{Ca} channel currents ($I_{BK(Ca)}$) cannot be recorded in isolation from $I_{K(DR)}$ because, as mentioned previously, there are no selective blockers of insect $I_{K(DR)}$. Therefore, to isolate $I_{BK(Ca)}$, 5 mM 4-AP was included in external recording solutions. Both 30 nM ChTx and 1 mM $CdCl_2$ were also perfused at the conclusion of current recordings to eliminate $I_{BK(Ca)}$ allowing for offline subtraction of the remaining $I_{K(DR)}$. While Cd^{2+} may modify many mammalian K_V channel currents there is no evidence to suggest that this is the case in DUM neurons. Unfortunately the use of ChTx, in the absence of Cd^{2+} , is insufficient to completely block BK_{Ca} channels and previous studies of BK_{Ca} channel blockers in DUM neurons have all found it necessary to employ Cd^{2+} to inhibit Ca^{2+} entry (Derst et al., 2003). In separate experiments, κ -TRTX-Ec2a, -Ec2b or -Ec2c were then perfused for a period of 10 minutes, or until equilibrium was achieved. 1 mM $CdCl_2$ and 30 nM ChTx were then applied to block BK_{Ca} channels. The remaining $I_{K(DR)}$, recorded in the presence of BK_{Ca} channel blockers, was then digitally subtracted from both control and currents recorded in the presence of each κ -TRTX-Ec2 toxin (Fig. 6B). All three toxins caused a similar concentration-dependent block of both transient and sustained $I_{BK(Ca)}$ at all concentrations tested. The IC_{50} values for block of $I_{BK(Ca)}$ by κ -TRTX-Ec2a, -Ec2b and -Ec2c were 3.7, 25.3 and 24.6 nM for peak $I_{BK(Ca)}$ and 3.7, 25.8 and 19.1 nM for late $I_{BK(Ca)}$, respectively (Fig. 7E, 7F). The *ca.* 6-fold higher potency of κ -TRTX-Ec2a *vs.* Ec2b/Ec2c on peak and late $I_{BK(Ca)}$ maybe partially explained by the significant block of $I_{K(DR)}$ by κ -TRTX-Ec2a (Figs. 5Ca, 5Da), which would cause an apparent increase in potency following $I_{K(DR)}$ subtraction routines in $I_{BK(Ca)}$ isolation procedures. Thus, while κ -TRTX-Ec2 toxins share considerable sequence homology with other spider toxins targeting Na_V , K_V or Ca_V channels, some of which are promiscuous in their actions on multiple families of ion channel (eg β/ω -TRTX-Tp2a), the evidence from the present study indicates that κ -TRTX-Ec2 toxins act selectively on BK_{Ca} channels.

To assess whether κ -TRTX-Ec2 toxins block DUM neuron BK_{Ca} channels in a voltage-dependent manner, the current-voltage ($I_{BK(Ca)}-V$) relationship in the presence of each toxin was determined. Families of $I_{BK(Ca)}$ were elicited by a series of 100 ms voltage pulses from a V_h of -80 mV to $+40$ mV

in 10-mV increments at a frequency of 0.2 Hz. The threshold of $I_{BK(Ca)}$ activation was at membrane potentials greater than -40 mV, which is in agreement with previous data from BK_{Ca} channel recordings in DUM neurons (Grolleau and Lapied, 1995; Gunning et al., 2008). In the presence of 6 nM κ -TRTX-Ec2a, 25 nM κ -TRTX-Ec2b or 25 nM κ -TRTX-Ec2c there was no shift in the threshold or $V_{1/2}$ of $I_{BK(Ca)}$ activation of either peak or late $I_{BK(Ca)}$ (Fig. 7). Further, channel block was not relieved at increasing potentials (Figs. 7Ac, 7Bc, 7Cc) as noted for other voltage-dependent toxins, including many theraphosid spider toxins (for a review see Swartz, 2007).

Discussion

κ -TRTX-Ec2 toxins target insect BK_{Ca}

Although all three of the κ -TRTX-Ec2 toxins share significant homology with a number of short-loop theraphotoxins acting on mammalian voltage-activated ion channels they are unique from two perspectives. Firstly, κ -TRTX-Ec2a and κ -TRTX-Ec2b are strictly insect-selective and thus show invertebrate phyla-selectivity not previously described for this group of toxins. Secondly, κ -TRTX-Ec2 toxins display high affinity and selectivity for the insect BK_{Ca} channel, a pharmacology previously only reported with κ -hexatoxin-Hv1c (Gunning et al., 2008), with whom they share no significant homology (Fig. 3B). As potent ligands for the insect BK_{Ca} channel, these toxins therefore represent valuable tools in the exploration of BK_{Ca} channel structure and characterizing the biological functions of insect BK_{Ca} channels. Indeed these two families of toxins may become the defining pharmacology for insect BK_{Ca} channels.

Mode of action

Several lines of evidence suggest that κ -TRTX-Ec2 toxins interact with their target via mechanisms unique from other theraphotoxins. Until the present study, K_v channel modulators from tarantula venoms were all characterised as gating-modifier toxins (for a review see Swartz, 2007). These toxins inhibit conductance by interfering with the voltage-sensing region of ion channels to cause a depolarizing shift in the voltage-dependence of activation thus stabilizing the closed or inactivated

states of the channel. However, unlike all other theraphotoxins acting on K_V channels, BK_{Ca} current inhibition induced by the κ -TRTX-Ec2 toxins failed to exhibit any depolarizing shifts in the threshold, or voltage midpoint ($V_{1/2}$), of channel activation clearly indicating that the mechanism of channel inhibition is not via modulation of channel gating.

Other toxins interacting with K_V channels block ion conduction by physically occluding the pore of the channel near the selectivity filter. 'Pore blockers' interact with amino acids situated in the S5-S6 linker and physically occlude the pore (Gross and MacKinnon, 1996). Among structurally dissimilar K_V channel pore blockers from sea anemone and scorpion venoms, a 'functional dyad' is common to the bioactive surface of the molecules. This comprises an invariant Lys residue situated within $6.6 \pm 1.0 \text{ \AA}$ of an aromatic residue such as Tyr or Phe (Dauplais et al., 1997). This mode of action is similar to that reported for the insect-selective neurotoxin κ -HXTX-Hv1c, from the venom of the hexathelid spider *Hadronyche versuta*, that also inhibits BK_{Ca} channels (Gunning et al., 2008). Homology modeling of κ -TRTX-Ec2 toxins on the known structure of κ -TRTX-Gr2a (formerly GsMTx-2 Oswald et al., 2002; PDB accession 1LUP), revealed several pairs of basic and aromatic residues that could satisfy the requirements of a functional dyad (Fig. 8). Possible functional dyads include Lys²⁶-Trp²⁴, Lys⁴-Phe⁵ (Lys⁵-Phe⁴ in κ -TRTX-Ec2c) and Lys¹⁴-Tyr¹. However, none of these potential dyads are unique from residues in other β - or β/ω -TRTX toxins that do not target K_V channels (Fig. 3A). Moreover, there was no apparent voltage-dependency to the degree of block at various membrane potentials, with no reduction in block at higher potentials. Classical pore blockers such as charybdotoxin (α -KTx 1.1), κ -conotoxin PVIIA and, to a lesser extent, κ -HXTX-Hv1c all demonstrate an alleviation of channel block at increasingly depolarised potentials as potassium driving force increases. Consequently these classical pore blockers all show moderate to strong voltage-dependent dissociation (Goldstein and Miller, 1993; Gunning et al., 2008; Terlau et al., 1999). Thus, the lack of voltage-dependent block by κ -TRTX-Ec2 toxins indicates that the toxins do not bind deeply into the extracellular mouth of the ion channel to plug the pore in a manner similar to other K_V and BK_{Ca} channel blockers.

Scorpion toxins that block small-conductance SK_{Ca} (K_{Ca2.x}) channels lack the conserved functional dyad present in peptide pore blockers of K_V, IK_{Ca} and BK_{Ca} channels. These toxins include, amongst others, scyllatoxin (α -KTx 5.1) and tamapin (α -KTx 5.4). Like κ -TRTX-Ec2 toxins, α -KTx 5.1 and α -KTx 5.4 have been shown to display a voltage-independent block of SK_{Ca} channels (Pedarzani et al., 2002; Shakkottai et al., 2001) and are believed to interact with the turret and loop region of the SK_{Ca} channel (Andreotti et al., 2005; Rodriguez de la Vega et al., 2003). Hence these types of toxins are known as ‘turret blockers’ to distinguish them from classical pore blockers. Unlike Lys²⁷ within the functional dyad of α -KTx 1.1, which plugs the pore of K_V and BK_{Ca} channels and senses approximately 20% of the transmembrane electrical field (Goldstein and Miller, 1993), these SK_{Ca} toxins and κ -TRTX-Ec2 toxins all lack a Lys²⁷-equivalent. Therefore we predict that κ -TRTX-Ec2 toxins, like α -KTx 5 toxins, are likely to bind to the extracellular channel surface and act as turret blockers to completely inhibit ion flux. There exists the possibility that κ -TRTX-Ec2 toxins act to block the channel by acting as an electrostatic barrier rather than via steric occlusion of the channel. However, other toxins that cause such a electrostatic inhibition of channels do not completely inhibit current flow, resulting in a residual current (Hui et al., 2002). Given that κ -TRTX-Ec2 toxins can completely inhibit BK_{Ca} channel currents, we believe that they cause a direct steric occlusion of the channel.

Structure and function

While the key residues comprising the bioactive surface (pharmacophore) of κ -TRTX-Gr2a are currently unknown, the pharmacophore of the highly homologous β/ω -TRTX-Tp2a (formerly ProTx-II) for Na_V channels has recently been identified (Smith et al., 2007). Comparing the pharmacophore of the Na_V and Ca_V channel-selective β/ω -TRTX-Tp2a (Fig. 8A) and the surface of the K_V4-selective κ -TRTX-Gr2a and κ -TRTX-Cj2a (Fig. 8B and C) with BK_{Ca} selective κ -TRTX-Ec2 toxins it can be seen that the major surface residues that differ for κ -TRTX-Ec2 toxins are located at the C-terminal region (particularly residues 28–29), with additional mutations at positions 4–6, 11, 18 and 22 (Fig. 8D-F). In particular, the presence of a Glu residue at either position 28 or 29 in κ -TRTX-Ec2a and κ -

TRTX-Ec2b is likely to confer insect-selectivity, as all of the remaining mammalian-active theraphotoxins have a basic or hydrophobic residue at one, or both, of these positions (Fig. 3A). Furthermore, affinity for the BK_{Ca} channel displayed by κ -TRTX-Ec2 toxins is likely to result from substitutions in the highly conserved Lys⁴-Trp⁵-Met⁶ of short-loop theraphotoxins (Fig. 3A), particularly as the apparent spatial location of Lys⁴-Phe⁵ of κ -TRTX-Ec2a and κ -TRTX-Ec2b (Phe⁴-Lys⁵ in κ -TRTX-Ec2c) is different from the other theraphotoxins (Fig. 8).

Importantly, differences in the sequence of the K_v/BK_{Ca} channel target can also drastically alter the affinity of toxins for the channel complex. While the selectivity filter and pore helix are well conserved across all potassium channels, the solvent-exposed turret and loop regions display high sequence variability and contribute to differences in α -KTx specificity (Giangiacomo et al., 2008). This can also extend to a variation in the size of the turret region. For example, the BK_{Ca} (Slo1) channel turret has six more residues with very limited sequence homology to the turret region of K_v1 channels (Giangiacomo et al., 2008). The size and sequence variability of the BK_{Ca} channel turret and loop regions could therefore explain the high selectivity of κ -TRTX-Ec2 toxins for BK_{Ca} over K_v channels. These sequence and size variations in the turret region also extend to subtle differences between the turret regions of various BK_{Ca} channels across different phyla. While the size of the turret region of BK_{Ca} channels from vertebrates, marine invertebrates and nematodes is believed to be the same, insect BK_{Ca} turret regions are typically 1-3 amino acids shorter (Giangiacomo et al., 2008; Gunning et al., 2008). Furthermore, single point mutations in this region can result in dramatic changes in the phyletic selectivity of toxins (Derst et al., 2003; Myers and Stampe, 2000). Thus, the amino acid variation in the turret and loop regions of insect vs. vertebrate BK_{Ca} channels appears sufficient to explain the insect selectivity of κ -TRTX-Ec2 toxins and κ -HXTX-Hv1c (Gunning et al., 2008).

Importantly, subtle changes in toxin sequence can also drastically alter the affinity of the toxin for specific channel subtypes. For example, point mutations of Lys³² in α -KTx 1.1 result in mutants with markedly reduced affinity for K_v1.2 and K_v1.3 channels but little change in affinity for BK_{Ca} or IK_{Ca} channels (Rauer et al., 2000). In addition, a chimeric toxin construct involving residues from the α/β

turn of iberiotoxin (α -KTx 1.3) grafted into noxiustoxin (α -KTx 2.1) causes a 50-fold weaker block of $K_v1.3$ channels, but a >150-fold higher affinity for block of BK_{Ca} channels (Mullmann et al., 2001). These variations highlight that subtle differences in toxin sequence can have profound effects on channel subtype selectivity or specificity. This, together with variations in the amino acid sequence of channel subtypes, likely explains the different pharmacologies and modes of action of BK_{Ca} -selective κ -TRTX-Ec2 toxins vs. other short-loop theraphosid spider toxins.

Novel lead compounds that validate new insecticide targets

The κ -TRTX-Ec2 toxins represent the second family of toxins, along with κ -HXTX-Hv1c, to validate insect BK_{Ca} channels as potential targets for insecticides. As potent and selective blockers of insect BK_{Ca} channels, κ -TRTX-Ec2a and κ -TRTX-Ec2b toxins also represent valuable lead compounds in the development of future insect-selective biopesticides with a novel mode of action. Nevertheless, in order to undertake any structure-based rational insecticide design program there is also a need to identify the residues responsible for phyla and target selectivity. Therefore the close sequence homology between diverse short-loop theraphotoxins, displaying both phyla-selective neurotoxicity and diverse pharmacology, has afforded the unique opportunity to hypothesize on the molecular determinants for insecticidal and target selectivity. As a result future mutagenesis experiments to determine the pharmacophore of the κ -TRTX-Ec2 toxins, guided by these hypotheses, should enable the determination of the residues responsible for insect selectivity and assist in the design of phyla-selective peptidomimetic insecticidal compounds.

Authorship Contributions

Participated in research design: Windley, Escoubas, Valenzuela, and Nicholson.

Conducted experiments: Windley, Escoubas, and Nicholson.

Contributed new reagents or analytic tools: N/A.

Performed data analysis: Windley, Escoubas, and Nicholson.

Wrote or contributed to the writing of the manuscript: Windley, Escoubas, Valenzuela, and Nicholson.

References

- Andreotti N, di Luccio E, Sampieri F, De Waard M and Sabatier J-M (2005) Molecular modeling and docking simulations of scorpion toxins and related analogs on human SKCa2 and SKCa3 channels. *Peptides* **26**(7):1095-1108.
- Chong Y, Hayes JL, Sollod B, Wen S, Wilson DT, Hains PG, Hodgson WC, Broady KW, King GF and Nicholson GM (2007) The ω -atracotoxins: selective blockers of insect M-LVA and HVA calcium channels. *Biochem Pharmacol* **74**(4):623-638.
- Corzo G, Diego-García E, Clement H, Peigneur S, Odell G, Tytgat J, Possani LD and Alagón A (2008) An insecticidal peptide from the therapsid *Brachypelma smithi* spider venom reveals common molecular features among spider species from different genera. *Peptides* **29**:1901-1908.
- Dauplais M, Lecoq A, Song J, Cotton J, Jamin N, Gilquin B, Roumestand C, Vita C, Medeiros CLCd, Rowan EG, Harvey AL and Ménez A (1997) On the convergent evolution of animal toxins. Conservation of a diad of functional residues in potassium channel-blocking toxins with unrelated structures. *J Biol Chem* **272**:4302-4309.
- Derst C, Messutat S, Walther C, Eckert M, Heinemann SH and Wicher D (2003) The large conductance Ca^{2+} -activated potassium channel (pSlo) of the cockroach *Periplaneta americana*: structure, localization in neurons and electrophysiology. *Eur J Neurosci* **17**(6):1197-1212.
- Diochot S, Drici M-D, Moinier D, Fink M and Lazdunski M (1999) Effects of phrixotoxins on the Kv4 family of potassium channels and implications for the role of I_{to1} in cardiac electrogenesis. *Br J Pharmacol* **126**(1):251-263.
- Edgerton GB, Blumenthal KM and Hanck DA (2007) Modification of gating kinetics in $Ca_v3.1$ by the tarantula toxin ProTxII, in *2007 Biophysical Society Meeting* pp 2865-Pos, Baltimore, Maryland.
- Escoubas P (2006) Molecular diversification in spider venoms: a web of combinatorial peptide libraries. *Mol Divers* **10**(4):545-554.
- Escoubas P and Rash LD (2004) Tarantulas: eight-legged pharmacists and combinatorial chemists. *Toxicon* **43**(5):555-574.
- Escoubas P, Sollod B and King GF (2006) Venom landscapes: mining the complexity of spider venoms via a combined cDNA and mass spectrometric approach. *Toxicon* **47**(6):650-663.
- Giangiaco KM, Becker J, Garsky C, Schmalhofer W, Garcia M and Mullmann TJ (2008) Novel α -KTx sites in the BK channel and comparative sequence analysis reveal distinguishing features of the BK and KV channel outer pore. *Cell Biochem Biophys* **52**(1):47-58.
- Goldstein SA and Miller C (1993) Mechanism of charybdotoxin block of a voltage-gated K^+ channel. *Biophys J* **65**(4):1613-1619.

- Grolleau F and Lapied B (1995) Separation and identification of multiple potassium currents regulating the pacemaker activity of insect neurosecretory cells (DUM neurons). *J Neurophysiol* **73**(1):160-171.
- Gross A and MacKinnon R (1996) Agitoxin footprinting the shaker potassium channel pore. *Neuron* **16**(2):399-406.
- Gunning SJ, Maggio F, Windley MJ, Valenzuela SM, King GF and Nicholson GM (2008) The Janus-faced atracotoxins are specific blockers of invertebrate K_{Ca} channels. *FEBS J* **275**:4045-4059.
- Herzig V, Wood DLA, Newell F, Chaumeil P-A, Kaas Q, Binford GJ, Nicholson GM, Gorse D and King GF (2011) ArachnoServer 2.0, an updated online resource for spider toxin sequences and structures. *Nucleic Acids Research* **39**(Suppl1):D653-D657.
- Hui K, Lipkind G, Fozzard HA and French RJ (2002) Electrostatic and steric contributions to block of the skeletal muscle sodium channel by μ -conotoxin. *J Gen Physiol* **119**(1):45-54.
- King GF (2007) Modulation of insect Ca_v channels by peptidic spider toxins. *Toxicon* **49**(4):513-530.
- King GF, Escoubas P and Nicholson GM (2008a) Peptide toxins that selectively target insect Na_v and Ca_v channels. *Channels (Austin, Tex)* **2**(2):100-116.
- King GF, Gentz MC, Escoubas P and Nicholson GM (2008b) A rational nomenclature for naming peptide toxins from spiders and other venomous animals. *Toxicon* **52**(2):264-276.
- Li D, Xiao Y, Hu W, Xie J, Bosmans F, Tytgat J and Liang S (2003) Function and solution structure of hainantoxin-I, a novel insect sodium channel inhibitor from the Chinese bird spider *Selenocosmia hainana*. *FEBS Lett* **555**(3):616-622.
- Maggio F and King GF (2002) Scanning mutagenesis of a Janus-faced atracotoxin reveals a bipartite surface patch that is essential for neurotoxic function. *J Biol Chem* **277**(25):22806-22813.
- Middleton RE, Warren VA, Kraus RL, Hwang JC, Liu CJ, Dai G, Brochu RM, Kohler MG, Gao YD, Garsky VM, Bogusky MJ, Mehl JT, Cohen CJ and Smith MM (2002) Two tarantula peptides inhibit activation of multiple sodium channels. *Biochemistry* **41**(50):14734-14747.
- Mullmann TJ, Spence KT, Schroeder NE, Fremont V, Christian EP and Giangiacomo KM (2001) Insights into α -K toxin specificity for K⁺ channels revealed through mutations in noxiustoxin. *Biochemistry* **40**(37):10987-10997.
- Myers MP and Stampe P (2000) A point mutation in the maxi-K clone dSlo forms a high affinity site for charybdotoxin. *Neuropharmacology* **39**(1):11-20.
- Nicholson GM (2007a) Fighting the global pest problem: preface to the special *Toxicon* issue on insecticidal toxins and their potential for insect pest control. *Toxicon* **49**(4):413-422.
- Nicholson GM (2007b) Insect-selective spider toxins targeting voltage-gated sodium channels. *Toxicon* **49**(4):490-512.
- Oswald RE, Suchyna TM, McFeeters R, Gottlieb P and Sachs F (2002) Solution structure of peptide toxins that block mechanosensitive ion channels. *J Biol Chem* **277**(37):34443-34450.

- Pallaghy P, Neilsen K, Craik D and Norton R (1994) A common structural motif incorporating a cystine knot and a triple-stranded β -sheet in toxic and inhibitory polypeptides. *Protein Sci* **3**:1833-1839.
- Pedarzani P, D'hoedt D, Doorty KB, Wadsworth JDF, Joseph JS, Jeyaseelan K, Kini RM, Gadre SV, Sapatnekar SM, Stocker M and Strong PN (2002) Tamapin, a venom peptide from the Indian red scorpion (*Mesobuthus tamulus*) that targets small conductance Ca^{2+} -activated K^+ channels and afterhyperpolarization currents in central neurons. *J Biol Chem* **277**(48):46101-46109.
- Rauer H, Lanigan MD, Pennington MW, Aiyar J, Ghanshani S, Cahalan MD, Norton RS and Chandy KG (2000) Structure-guided transformation of charybdotoxin yields an analog that selectively targets Ca^{2+} -activated over voltage-gated K^+ channels. *J Biol Chem* **275**(2):1201-1208.
- Rodriguez de la Vega RC, Merino E, Becerril B and Possani LD (2003) Novel interactions between K^+ channels and scorpion toxins. *TIPS* **24**(5):222-227.
- Salkoff L, Baker K, Butler A, Covarrubias M, Pak MD and Wei A (1992) An essential 'set' of K^+ channels conserved in flies, mice and humans. *TINS* **15**(5):161-166.
- Shakkottai VG, Regaya I, Wulff H, Fajloun Z, Tomita H, Fathallah M, Cahalan MD, Gargus JJ, Sabatier J-M and Chandy KG (2001) Design and characterization of a highly selective peptide inhibitor of the small conductance calcium-activated K^+ channel, SkCa2. *J Biol Chem* **276**(46):43145-43151.
- Smith JJ, Cummins TR, Alphy S and Blumenthal KM (2007) Molecular interactions of the gating modifier toxin ProTx-II with $\text{Nav}1.5$: implied existence of a novel toxin binding site coupled to activation. *J Biol Chem* **282**(17):12687-12697.
- Swartz KJ (2007) Tarantula toxins interacting with voltage sensors in potassium channels. *Toxicon* **49**(2):213-230.
- Terlau H, Boccaccio A, Olivera BM and Conti F (1999) The block of *Shaker* K^+ channels by κ -conotoxin PVIIA is state dependent. *J Gen Physiol* **114**(1):125-140.
- Wei A, Covarrubias M, Butler A, Baker K, Pak M and Salkoff L (1990) K^+ current diversity is produced by an extended gene family conserved in *Drosophila* and mouse. *Science* **248**(4955):599-603.
- Wicher D and Penzlin H (1997) Ca^{2+} currents in central insect neurons: electrophysiological and pharmacological properties. *J Neurophysiol* **77**(1):186-199.

Footnotes

¹**Current affiliation:** VenomeTech, 473 Route des Dolines, Sophia Antipolis, 06560 Valbonne, France

Financial Support Credit: This work was supported in part by an Australian Research Council Discovery Grant [Grant DP0559396 to G.M.N. and S.M.V.], a Department of Education, Science and Training – International Science Linkage Grant [Grant FR050106 to G.M.N.], a Centre National de la Recherche Scientifique - Projet International de Coopération Scientifique Grant [Grant 3603 to P.E.] and an Australian Postgraduate Award to M.J.W.

Legends for Figures

Fig. 1. Insecticidal toxicity screening of tarantula venoms in *Gryllus bimaculatus* crickets. ED₅₀ values for paralysis at 15 min post intra-thoracic injection were calculated by the probit method and are expressed as microliters of crude venom/g of insect. Values represent the mean ± 95% confidence limits with $n = 3$ in all cases, except species 36 and 37 where $n = 1$ due to lack of potency and availability of venom.

Fig. 2. Isolation and purification of κ -TRTX-Ec2 toxins. **(A)** C8 RP-HPLC of crude *E. constrictus* venom (20 μ l). Gradient: 0% B 5 min, 0–15% B 15 min, 15–50% B 70 min, 50–60% B 10 min, 60–90% B 5 min, 90–0% B 5 min. A = H₂O / 0.1% TFA, B = acetonitrile / 0.1% TFA, 2 ml/min. Eluted peptides were monitored at an absorbance of 215 nm. **(B)** Cation-exchange HPLC of pooled fractions 14–16 (f_{14}) from C8 RP-HPLC (shaded peaks in panel A). Gradient: 0% B 10 min, 0–50% B 50 min, 50–100% B 15 min, 100–0% B 15 min. A = 20 mM ammonium acetate, B = 2 M ammonium acetate, 0.5 ml/min. Eluted peptides were monitored at an absorbance of 280 nm. **(C)** C18 RP-HPLC purification of fractions $f_{14.2}$ (κ -TRTX-Ec2a, **Ca**), $f_{14.3}$ (κ -TRTX-Ec2b, **Cb**) and $f_{14.3}$ (κ -TRTX-Ec2c, **Cc**) from cation-exchange HPLC (shaded peaks in panel B). Gradient 0% B 5 min, 0–15% B 15 min, 15–40% B 50 min, 40–90% B 10 min, 90–0% B 5 min. A = H₂O / 0.1% TFA, B = acetonitrile / 0.1%TFA, 1 ml/min. Eluted peptides were monitored at an absorbance of 215 nm. In each panel retention times (in mins) are shown above each peak.

Fig. 3. Homology of κ -TRTX-Ec2 toxins with short-loop ICK spider toxins. **(A)** A Blast search was run through the ArachnoServer 2.0 Database highlighting peptides with highly homologous sequences. All sequences belong to the short-loop ICK group of tarantula toxins defined by three residues in the loop between the highlighted C_V and C_{VI} cysteine residues (Escoubas and Rash, 2004). Homologies are shown relative to κ -TRTX-Ec2a; identities are boxed in *gray* while conservative substitutions are in *gray italic* text. Stars represent C-terminal amidation. Percentage identity (%I) is relative to κ -TRTX-Ec2a while percentage homology (%H) includes conservatively substituted residues. The disulfide bonding pattern for the strictly conserved cysteine residues determined for κ -TRTX-Gr2a (Oswald et al., 2002) and κ -TRTX-Ps2a (Diochot et al., 1999) is indicated above the sequences; it is assumed

that the κ -TRTX-Ec2 toxins share the same disulfide bonding pattern. The known mammalian targets (unless otherwise indicated) of these spider toxins are identified on the right, with channels identified in brackets indicating only weak affinity. Those targets annotated with '?' indicate a likely target based on considerable homology with a toxin of known pharmacology (eg. κ -TRTX-Gr2b and κ -TRTX-Gr2c). Notably κ -TRTX-Ps2b and κ -TRTX-Gr2a possess identical sequences although they originate from unrelated species. Sequence, post-translational modifications, disulfide connectivity and pharmacological target data was obtained from the ArachnoServer 2.0 database. **(B)** Despite sharing a similar phyla and target selectivity, κ -TRTX-Ec2 toxins show only limited homology to κ -HXTX-Hv1c (Gunning et al., 2008). Gaps (dashes) have been inserted to maximize alignment.

Fig. 4. Effects of κ -TRTX-Ec2 toxins on whole-cell Na_V , Ca_V and macroscopic K_V channel currents in cockroach DUM neurons. **(A-B)** Representative superimposed current traces showing the lack of a significant effect of 330 nM κ -TRTX-Ec2 toxins on **(A)** Na_V channel currents, **(Ba)** LVA- Ca_V channel currents or **(Bb)** HVA- Ca_V channel currents. Note the block of all residual I_{Na} and I_{Ba} by 300 nM TTX and 1 mM Cd^{2+} , respectively. **(C)** Superimposed current traces demonstrating the typical effect of κ -TRTX-Ec2a **(Ca)** and κ -TRTX-Ec2c **(Cb)** on macroscopic K_V channel currents. **(D)** Depolarizing voltage test pulse protocols used to activate I_{Na} (delivered at 0.1 Hz), I_{Ba} (0.1 Hz) and macroscopic I_K (0.2 Hz).

Fig. 5. Actions of κ -TRTX-Ec2 toxins on $I_{K(A)}$ and $I_{K(DR)}$ in cockroach DUM neurons. Panels show the effects of 330 nM κ -TRTX-Ec2a (left-hand panels, **a**), 330 nM κ -TRTX-Ec2b (centre panels, **b**) and 330 nM κ -TRTX-Ec2c (right-hand panels, **c**), while the depolarizing voltage test pulse protocols used to elicit currents are shown in the far right panels. **(A-B)** $I_{K(A)}$ were isolated in the presence of 30 nM ChTx and 1 mM CdCl_2 , combined with current subtraction routines utilising 5 mM 4-AP (see Results for details). **(A)** Typical superimposed whole-cell $I_{K(A)}$ were evoked by voltage steps to +30 mV from -90 mV for 100 ms in the presence, and absence, of toxin. **(B)** Families of whole-cell $I_{K(A)}$ were elicited by depolarizing test pulses from -90 mV to +40 mV in 10-mV increments. The membrane potential was then plotted against peak $I_{K(A)}$ amplitude and fitted to Equation 1. No significant shift in the

threshold, or voltage-midpoint, of activation of $I_{K(A)}$ was observed in the presence of 330 nM κ -TRTX-Ec2a (**a**, $n = 3$), κ -TRTX-Ec2b (**b**, $n = 7$) or κ -TRTX-Ec2c (**c**, $n = 3$). (**C-D**) $I_{K(DR)}$ were isolated in the presence of 30 nM ChTx, 1 mM CaCl_2 and 5 mM 4-AP. (**C**) Typical superimposed whole-cell $I_{K(DR)}$ were evoked by voltage steps to +30 mV from -90 mV for 100 ms in the presence, and absence, of toxin. (**D**) Families of whole-cell $I_{K(A)}$ were elicited by depolarizing test pulses from -90 mV to +40 mV in 10-mV increments. The membrane potential was then plotted against late current amplitude measured at 100 ms and data fitted to Equation 1. No shift in the threshold, or voltage-midpoint, of activation of $I_{K(DR)}$ occurred in the presence of 330 nM κ -TRTX-Ec2a (**a**, $n = 3$), κ -TRTX-Ec2b (**a**, $n = 3$) and κ -TRTX-Ec2c (**a**, $n = 7$). Data in panels (**B**) and (**D**) are expressed as the mean \pm standard error, ** $p < 0.01$.

Fig. 6. κ -TRTX-Ec2 toxins block BK_{Ca} channel currents. (**A**) Whole-cell $I_{\text{BK}(\text{Ca})}$ were recorded using the voltage test pulse protocol shown in panel **A**. Cells were held at -80 mV and stepped to +30 mV for a duration of 100 ms. (**B**) Current subtraction routine used to isolate BK_{Ca} channel currents (see Materials and Methods). (**C-E**) Typical effects of κ -TRTX-Ec2a, -Ec2b and -Ec2c are shown in panels (**C**), (**D**) and (**E**), respectively. Superimposed traces represent approximately 50% block of current (**a**) and close to complete block (**b**). (**F**) Concentration-response curves for inhibition of $I_{\text{BK}(\text{Ca})}$ by κ -TRTX-Ec2 toxins measured from (**Fa**) 'fast-transient' $I_{\text{BK}(\text{Ca})}$ (maximum peak outward current; circle in panel Ca), and (**Fb**) 'late-sustained' $I_{\text{BK}(\text{Ca})}$ (measured at 100 ms; square in panel Ca). Data in panel **F** were fitted to Equation 2 and are expressed as the mean \pm standard error ($n = 3-6$).

Fig. 7. Effects of κ -TRTX-Ec2 toxins on the voltage-dependence of BK_{Ca} channel activation in cockroach DUM neurons. Families of whole-cell $I_{\text{BK}(\text{Ca})}$ were elicited by depolarizing voltage test pulses from -80 to +40 mV in 10-mV increments from a holding potential of -80 mV (see voltage test pulse protocol in the inset of panel **Ac**). Whole-cell $I_{\text{BK}(\text{Ca})}/V$ relationships were recorded before (closed circles), and after (open circles), perfusion with (**A**) 6 nM κ -TRTX-Ec2a, (**B**) 25 nM κ -TRTX-Ec2b and (**C**) 25 nM κ -TRTX-Ec2c ($n = 3-4$). Measurements were taken from both (**a**) fast-transient, and (**b**) late-sustained $I_{\text{BK}(\text{Ca})}$ and fitted to Equation 1. No significant shifts in the voltage dependence of channel activation were observed. The right-hand column (**c**) shows the voltage dependence of the

fractional block of fast-transient $I_{BK(Ca)}$ for κ -TRTX-Ec2 toxins ($n = 3-4$), taken from data in panels Aa-Ca. Data were expressed as the mean \pm standard error and fitted using linear regression.

Fig. 8. Homology modelling of κ -TRTX-Ec2 toxins. All surface representations were modelled on the known NMR structure of the $K_v4.2/K_v4.3$ -selective toxin κ -TRTX-Gr2a (Panel **B**; PDB accession code 1LUP) using the automated protein homology-modelling server SWISS-MODEL. For each toxin, the right-hand structure has been rotated 180° about the y -axis. The coloured regions on the surfaces represent basic, positively-charged (blue), acidic, negatively charged (red), non-polar, hydrophobic (green) and polar, non-charged (yellow) residues. (**A**) Surface representation of the Na_v - and $Ca_v1.3/Ca_v3.1$ -selective β/ω -TRTX-Tp2a with the known pharmacophore residues for activity on $Na_v1.5$ channels highlighted (residues bounded by solid lines; Smith et al., 2007). N- and C-termini are also shown. (**C-F**) Putative structures of the $K_v4.1$ -selective κ -TRTX-Cj2a and the three BK_{Ca} -selective κ -TRTX-Ec2 toxins. Along with κ -TRTX-Gr2a, these structures depict key amino acids that are different from topologically equivalent residues in the pharmacophore of β/ω -TRTX-Tp2a (residues bounded by dotted lines). Surface representations were constructed using PYMOL for Macintosh v1.3.

Figure 1

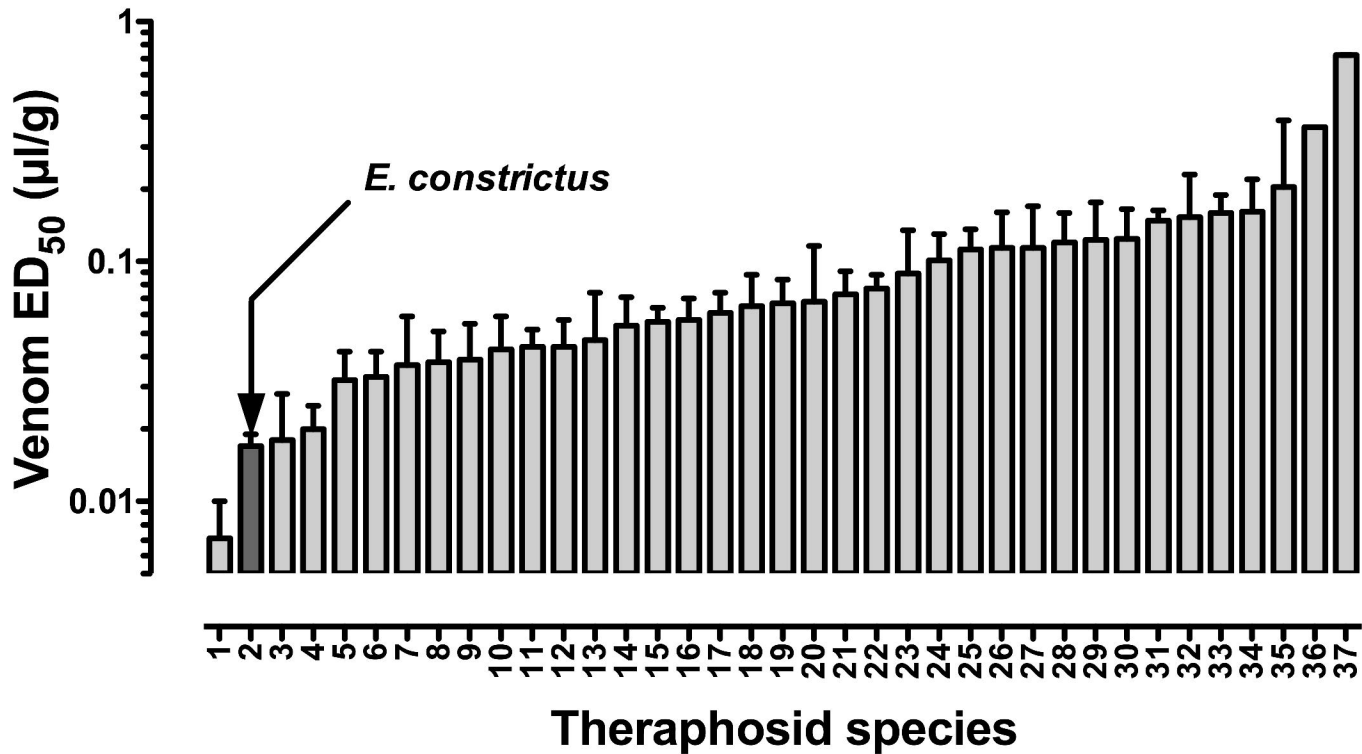


Figure 2

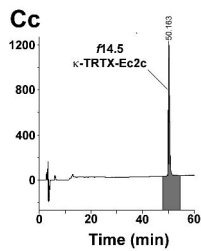
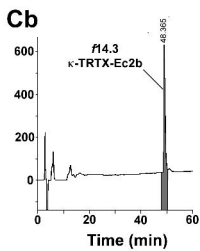
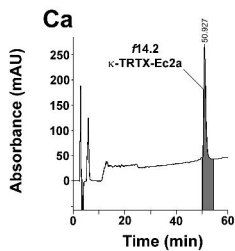
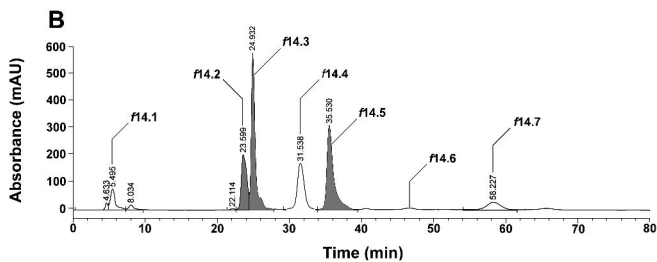
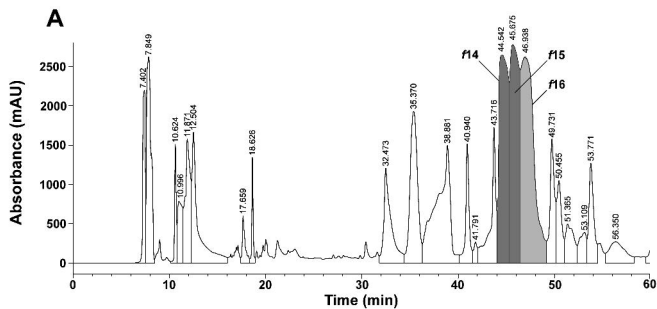
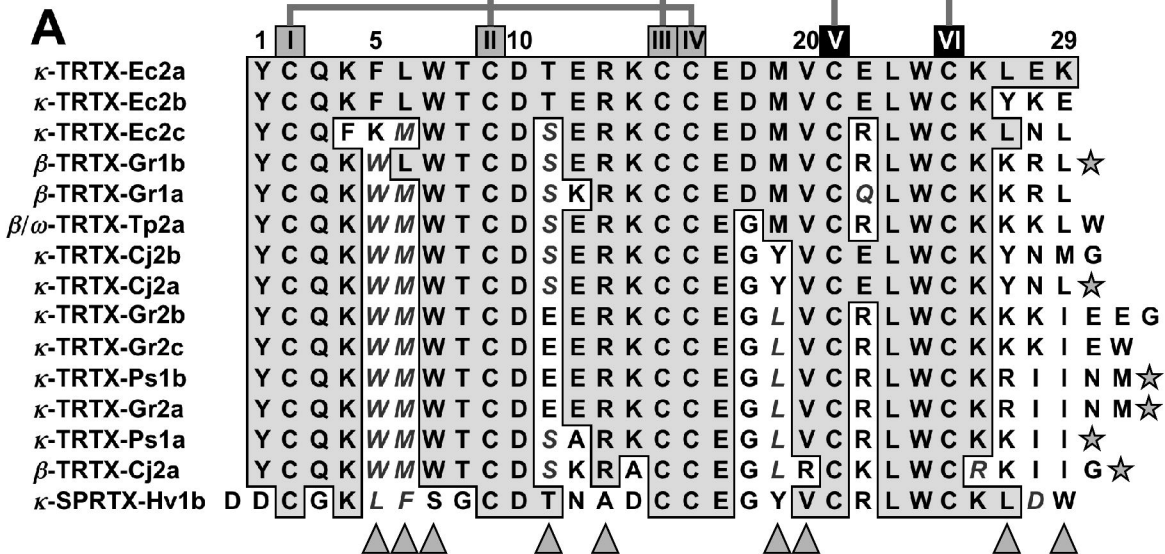
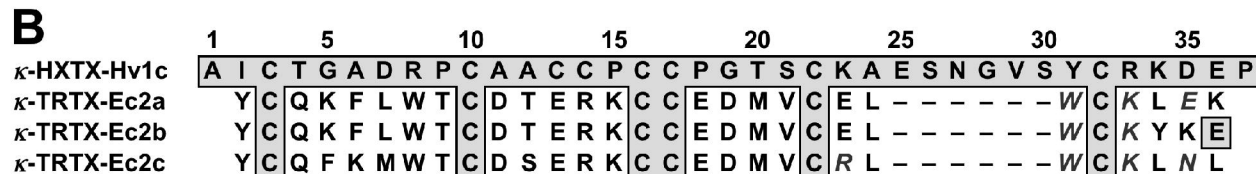


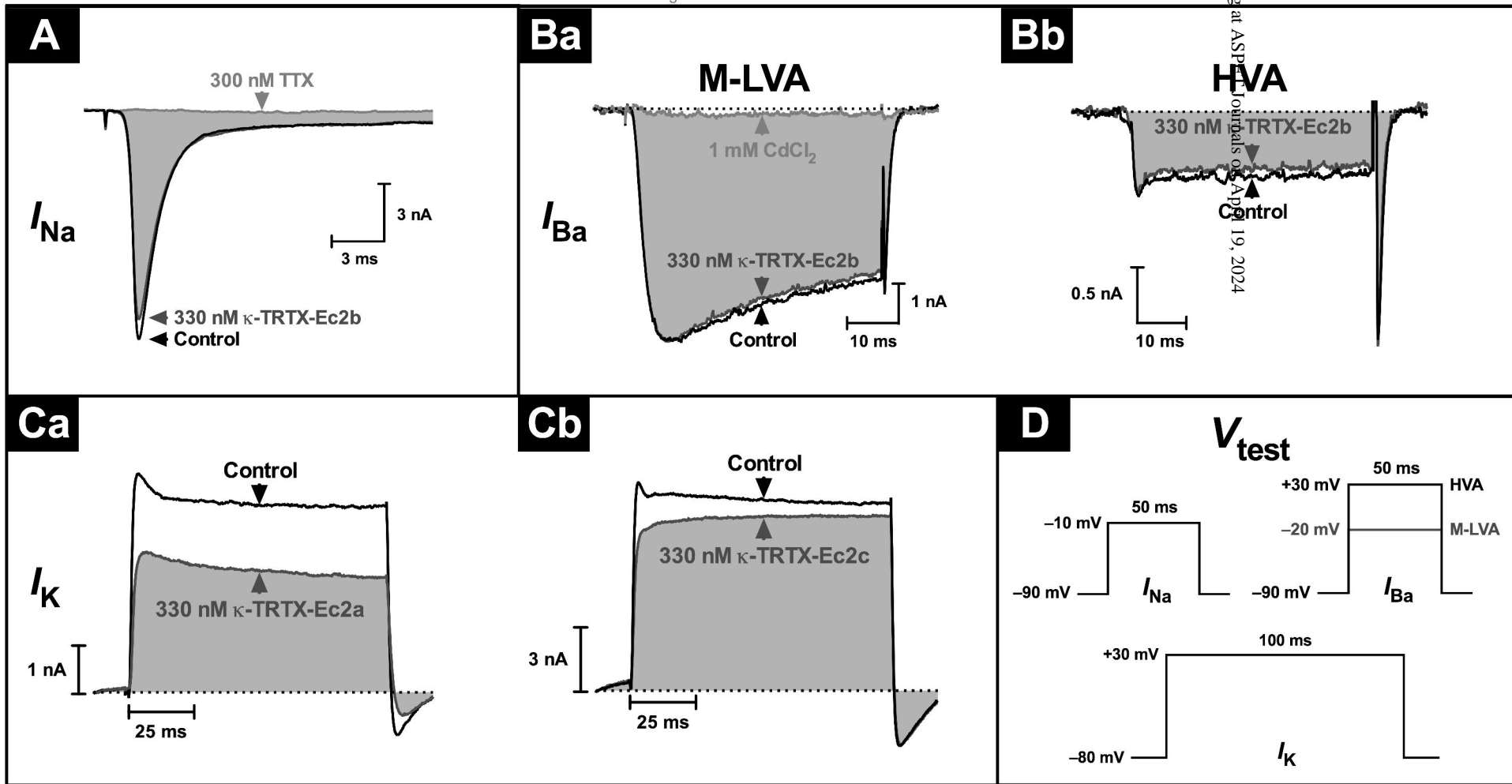
Figure 3

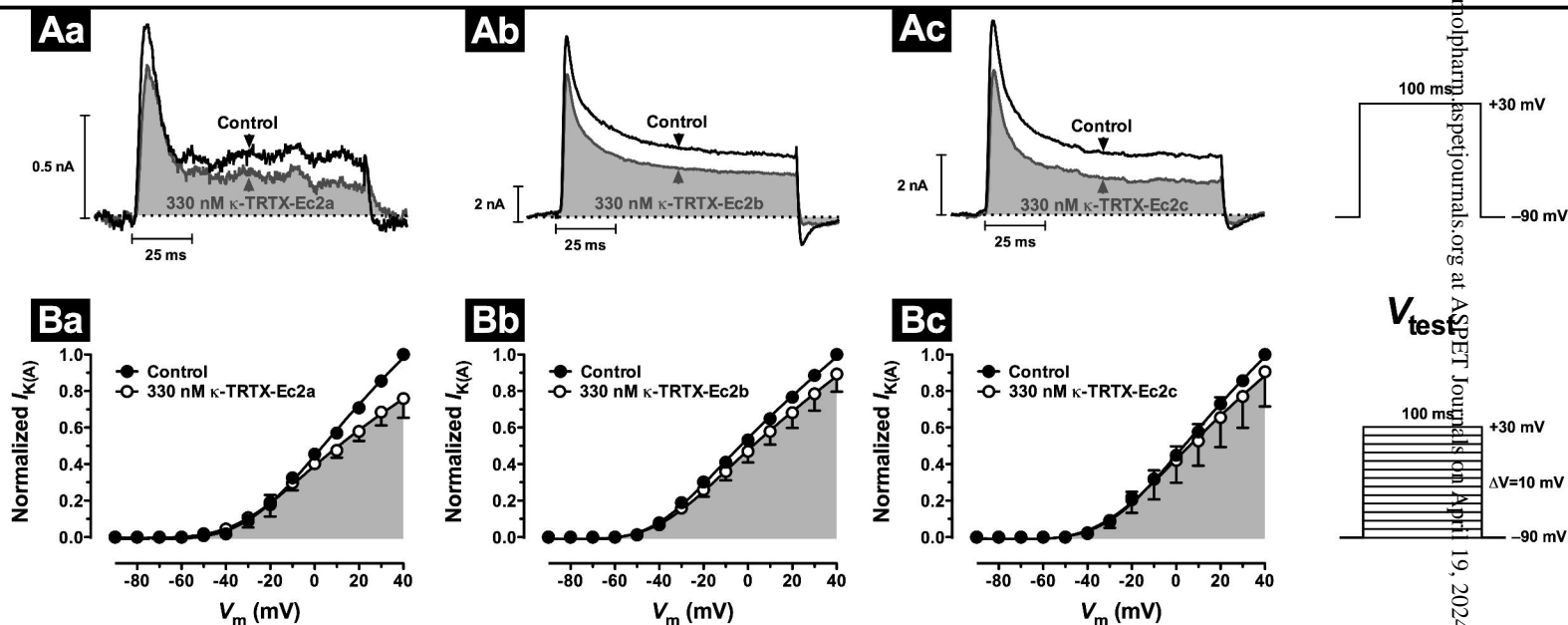
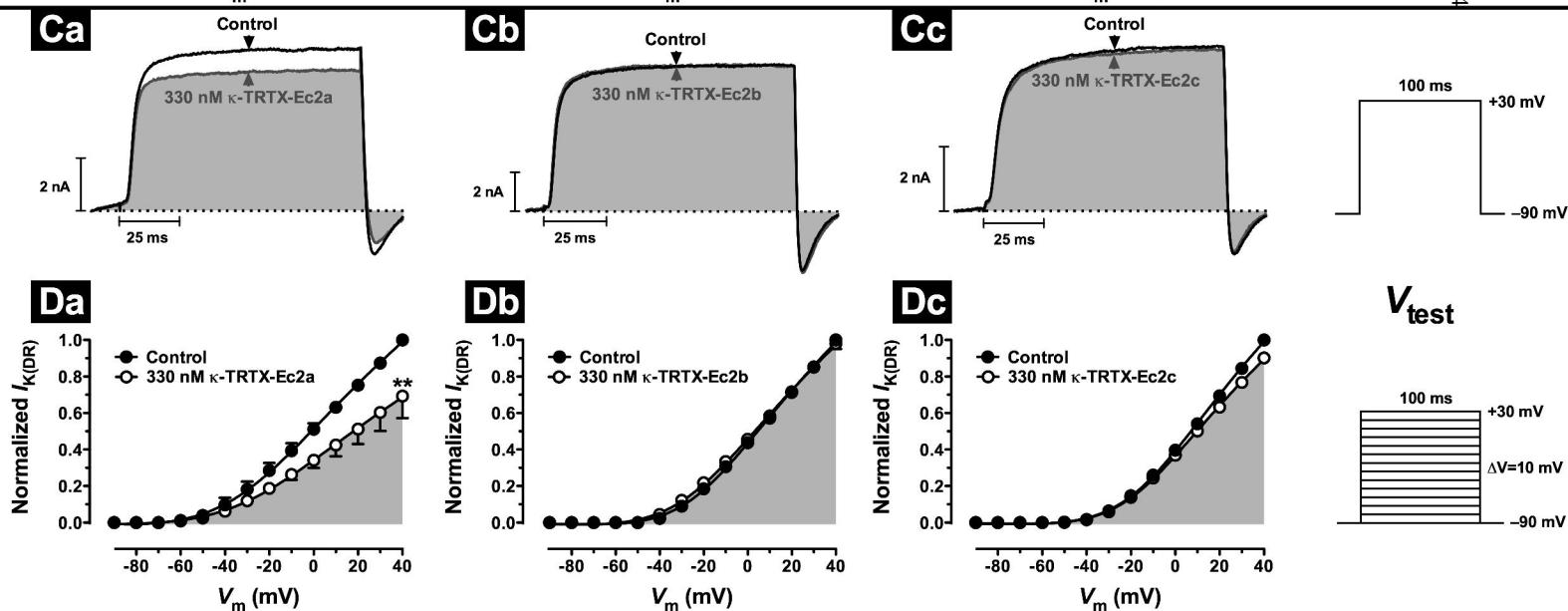


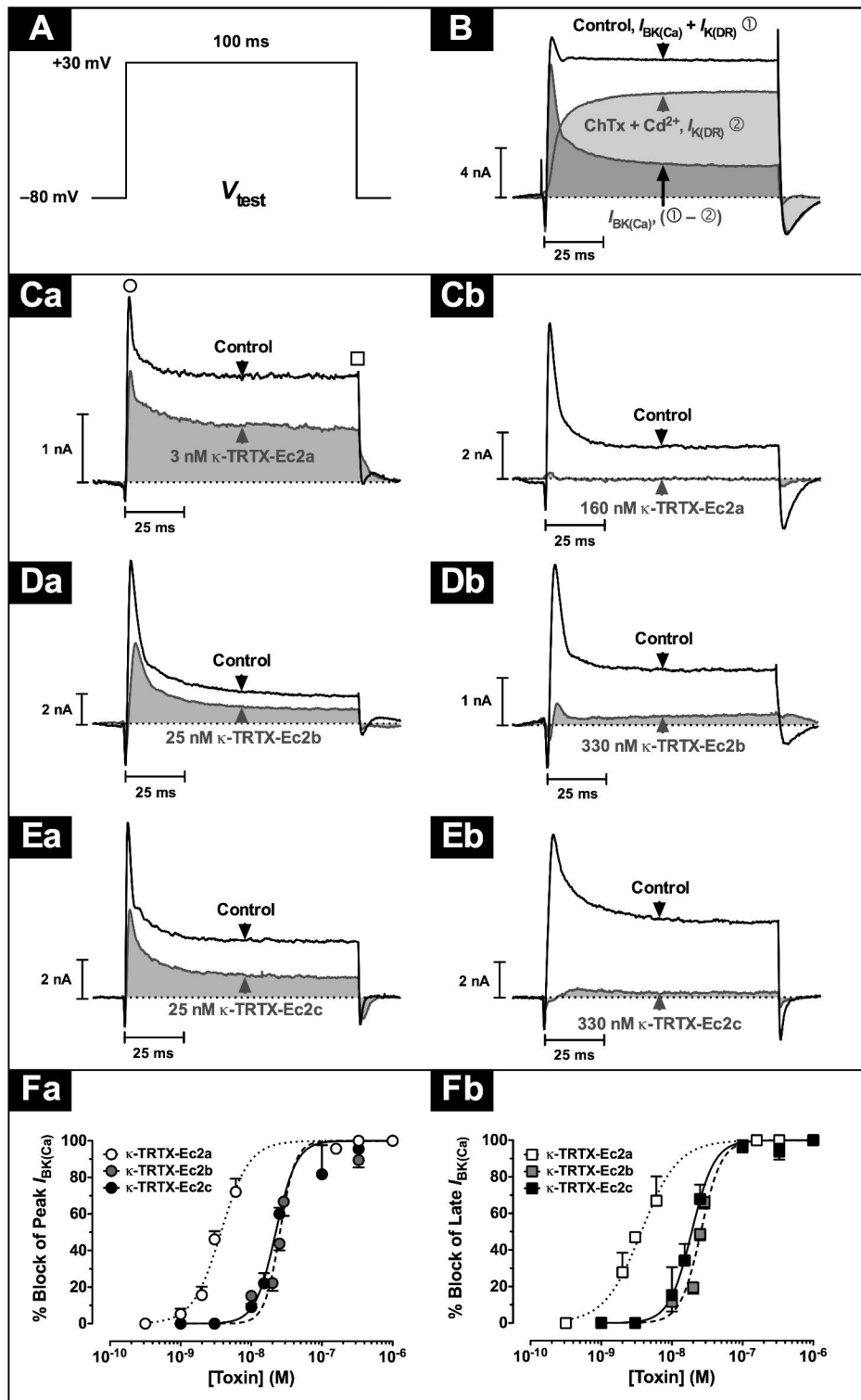
% I	% H	Target	Former Name	Source
100	100	BK _{Ca} (K _{DR}) insect	–	<i>E. constrictus</i>
90	90	BK _{Ca} insect	–	<i>E. constrictus</i>
76	83	BK _{Ca} insect	–	<i>E. constrictus</i>
79	86	Na _v	GsAFI	<i>Grammostola rosea</i>
72	86	Na _v	GrTx1	<i>Grammostola rosea</i>
72	83	Na _v , Ca _v 1.2, Ca _v 3.1	ProTx-II	<i>Thrixopelma pruriens</i>
72	83	K _v 4.1 (K _v 4.2, K _v 2.1)?	JZTX-46	<i>Chilobrachys jingzhao</i>
72	83	K _v 4.1 (K _v 4.2, K _v 2.1)	JZTX-XII	<i>Chilobrachys jingzhao</i>
69	80	K _v AP (MSC?)	VSTX2	<i>Grammostola rosea</i>
69	80	K _v AP? (MSC)	GsAFII	<i>Grammostola rosea</i>
69	80	K _v 4.2, K _v 4.3 (MSC)	PaTx2	<i>Paraphysa scrofa</i>
69	80	K _v 4.2, K _v 4.3 (MSC)	GsMTx-2	<i>Grammostola rosea</i>
66	80	K _v 4.2, K _v 4.3	PaTx1	<i>Paraphysa scrofa</i>
55	72	Na _v (K _v 4.2, K _v 4.3)	JZTX-V	<i>Chilobrachys jingzhao</i>
52	62	K _v 4.2, K _v 4.3 (K _v 4.1)	HPTX2	<i>Heteropoda venatoria</i>



% H	Target	Former Name	Source
100	BK _{Ca} (K _A) insect	J-ACTX-Hv1c	<i>Hadronyche versuta</i>
31	BK _{Ca} (K _{DR}) insect	–	<i>E. constrictus</i>
31	BK _{Ca} insect	–	<i>E. constrictus</i>
34	BK _{Ca} insect	–	<i>E. constrictus</i>



A-type, transient I_K Delayed-rectifier I_K 



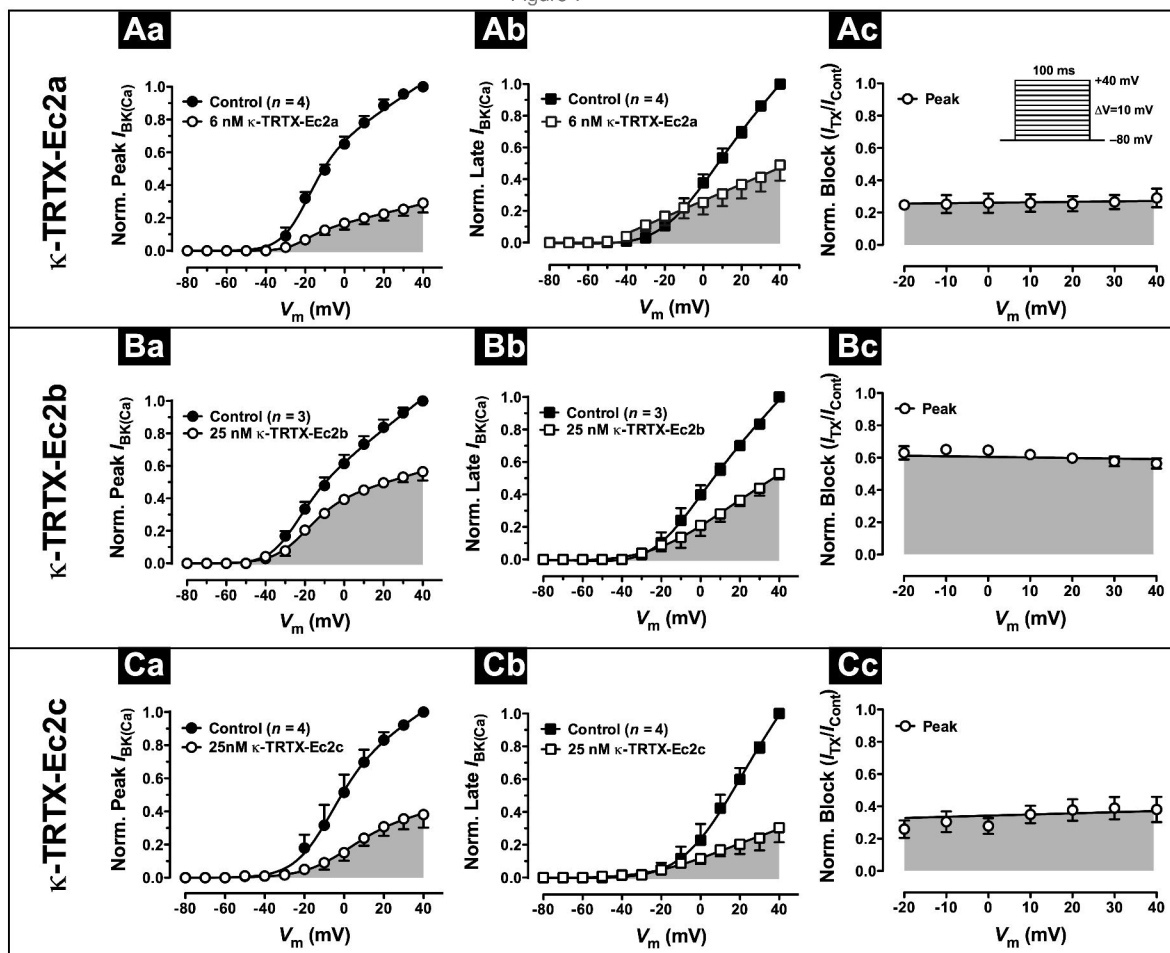


Figure 8

